Spectral hole burning and holography in an $Y_2SiO_5:Pr^{3+}$ crystal

Keith Holliday,* Mauro Croci, Eric Vauthey,† and Urs P. Wild
Physical Chemistry Laboratory, Swiss Federal Institute of Technology, ETH Zentrum, CH-8092, Zürich, Switzerland
(Received 19 October 1992; revised manuscript received 3 February 1993)

Holographic detection of spectral holes is demonstrated in a crystalline host material with signal-to-noise ratios of up to 10^4. Hole burning occurs in two Pr^{3+} sites in the Y_2SiO_5 lattice, in both cases due to population redistribution between the ground-state quadrupole levels. The signal contains contributions due to a resonant hole and several side holes and antiholes, a phenomenon not previously observed using the holographic technique. The diffracted spectrum is modeled in two ways. In the first case the transmission spectrum is used to determine the population gratings and thus the diffraction efficiency. In the second case the transition probabilities between ground- and excited-state Kramer's doublets are used to model the population gratings. The technique is applied to pseudo-Stark-effect measurements from which the crystallographic sites as determined by x-ray analysis are matched to the spectroscopic data presented here. The time decay of the diffracted signal is used to study nuclear spin-lattice relaxation. It is shown that at 1.6 K temperature-dependent phonon-induced processes make no contribution to this decay. The nonexponential time decay of the population upon radio-frequency irradiation resonant with a ground-state quadrupole splitting is attributed to Pr-Pr cross relaxation.

I. INTRODUCTION

Spectral hole burning involves the frequency-selective bleaching of an inhomogeneously broadened electronic transition of an impurity chromophore in a solid host.[1,2] Plane-wave holography is a method which may be used to detect weak spectral holes and has the advantage of being a zero background technique in that there is no diffracted signal outside the range of the hole profile.[3] The requirements that the hole-burning material has both excellent optical quality and strong electronic absorption have restricted the holographic technique to use with dye-doped polymers until now (though diffracted signals from persistent gratings produced as spectral holes in crystals have been detected using heterodyne techniques previously[4]). High-resolution spectroscopic studies of several dye-doped polymers have been performed using the combination of spectral hole burning and holography to obtain information on molecular parameters[5] and solvation effects.[6] Technological applications, which have been demonstrated in principle, include large scale frequency multiplexed image storage[7] and parallel processed data manipulation.[8] Here we report the application of plane-wave holography to a crystalline material, $Y_2SiO_5:Pr^{3+}$, for which a resonant hole and nonresonant side holes and antiholes are observed. The host material is of particular interest for optical data storage applications as its component ions have small proportions of magnetic isotopes and the nuclear magnetic moments of these are small.[9] The longest recorded optical dephasing time has been measured using Y_2SiO_5 as a host but with Eu^{3+} as the impurity.[10]

Spectral holes may often be produced in the zero-phonon $4f$ electronic transitions of lanthanide ion impurities in crystalline hosts.[11] The most common hole-burning mechanism is an optical pumping cycle which redistributes the ground-state population amongst the ground-state hyperfine levels. This results in a resonant spectral hole accompanied by a pattern of side holes and antiholes with spacings determined by the ground- and excited-state splittings.[12] These spectral features decay at a rate determined by the spin-lattice relaxation time.

The only naturally occurring isotope of praseodymium has a nuclear spin of $\frac{5}{2}$. The low-symmetry crystal field quenches orbital angular momentum and first-order hyperfine interactions are therefore forbidden. It has been shown[13] that the pure nuclear quadrupole interaction[14] and the second-order hyperfine induced "pseudo-quadrupole" interaction[13] may be combined to give the total nuclear quadrupole spin Hamiltonian for an electronic singlet,

$$\mathcal{H}_Q = D[I_{z''}^2 - I(I+1)/3] + E(I_{x''}^2 - I_{y''}^2) , \quad (1)$$

which is diagonalized in the x'', y'', z'' axis system. The combined coupling constants are given by D and E and the nuclear spin by I. The electronic singlets are split into three Kramers doublets and, due to the low site symmetry, the nuclear wave functions are mixed, causing the $\Delta m = 0$ selection rule to break down for electric dipole transitions between electronic singlets. Optical excitation and subsequent relaxation may thus result in a nuclear spin flip, causing a change of ground-state energy. Due to inhomogeneous broadening, each ion may have any one of the nine combinations of ground- and excited-state Kramer's doublets in resonance with the laser. Each of the nine sets makes a different contribution to the hole pattern the sum of which comprises of a resonant hole, six side holes and 42 antiholes.[12]

II. EXPERIMENTAL

Hole-burning spectra were recorded as both transmitted and diffracted intensities. A Coherent 699-21 ring

dye laser, stabilized to a linewidth of less than 1 MHz, operating with rhodamine 6G provided a beam of light resonant with the optical transition of interest. The laser output was split into two beams of equal intensity and recombined on the sample. The beams had a diameter of about 1 mm at the sample and a total power of about 200 μW whilst burning and 1 μW during reading. A typical burn time was 1 s. These powers facilitated good transmission and diffracted signals though holographic signals could still be detected with burn powers attenuated by a factor of 100. An increase in power by a factor of about 10 resulted in the spectral features broadening. This regime was therefore avoided.

The interference fringes create absorption and refractive index gratings due to spatially selective hole burning. Subsequent irradiation with one of the beams causes some of the light to be diffracted colinear with the other. By scanning the probe-laser frequency the diffracted and transmitted profiles of the spectral hole may be recorded simultaneously using a pair of photomultipliers and photon counting electronics. The experimental arrangement is shown in Fig. 1, the components of which have been described previously.[3] The experiment was controlled and data gathered and analyzed by a Sun Sparc Station 2 interfaced to a Stanford Research 400 two-channel gated photon counter via a National Instruments GPIB-SCSI controller.

The sample was a cylinder of 4-mm length and 8-mm diameter with window-glass-like optical quality. The praseodymium impurity concentration was 0.1 at. %. Electric fields could be applied by circular glass electrodes coated with a transparent conducting layer placed in contact with both flat faces. X-ray analysis showed that the perpendicular to the flat surfaces was 13° from a [010] axis. To prevent vibrations which would destroy phase stability for hologram production, the sample could not be rotated in any direction relative to the experimental frame.

Radio-frequency magnetic fields were applied to the sample via a copper coil of ten 10-mm turns with a vertically mounted axis, perpendicular to the laser propagation direction and parallel to the polarization of the laser. The radio frequency was generated by an Adret 7200 A signal generator and amplified by an Amplifier Research 100LMB radio-frequency amplifier, which produced a typical output of 1 W. This was delivered to the coil by means of a pair of stainless-steel coaxial cables and a high power 50-Ω terminator completed the circuit. The reflection from the coil was approximately 25%.

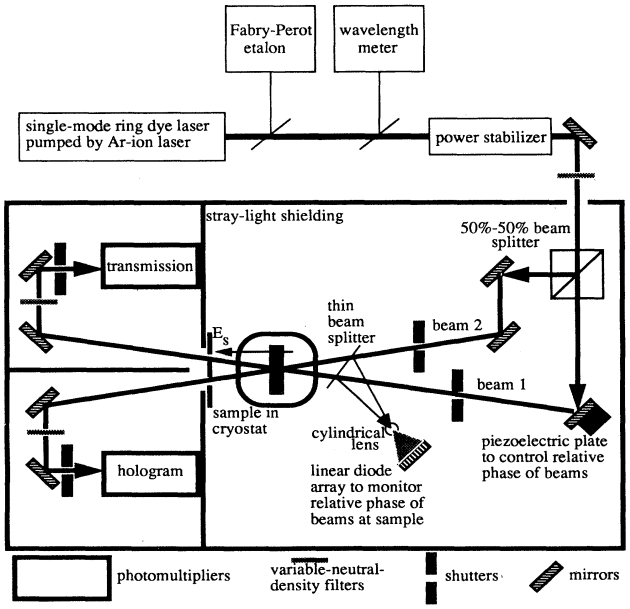

FIG. 1. The experimental arrangement used for spectral hole burning and holography. The direction of the externally applied electric field is indicated by E_s.

III. INHOMOGENEOUS SPECTRA

Spectroscopic measurements of Y_2SiO_5:Pr^{3+} have not previously been reported. However, it is known that when triply ionized rare-earth ions substitute for yttrium in Y_2SiO_5 crystals they occupy two sites, both of which have C_1 symmetry.[15] The $^3H_4$ ground state and the $^1D_2$ excited state are thus split by the crystal field into mani-

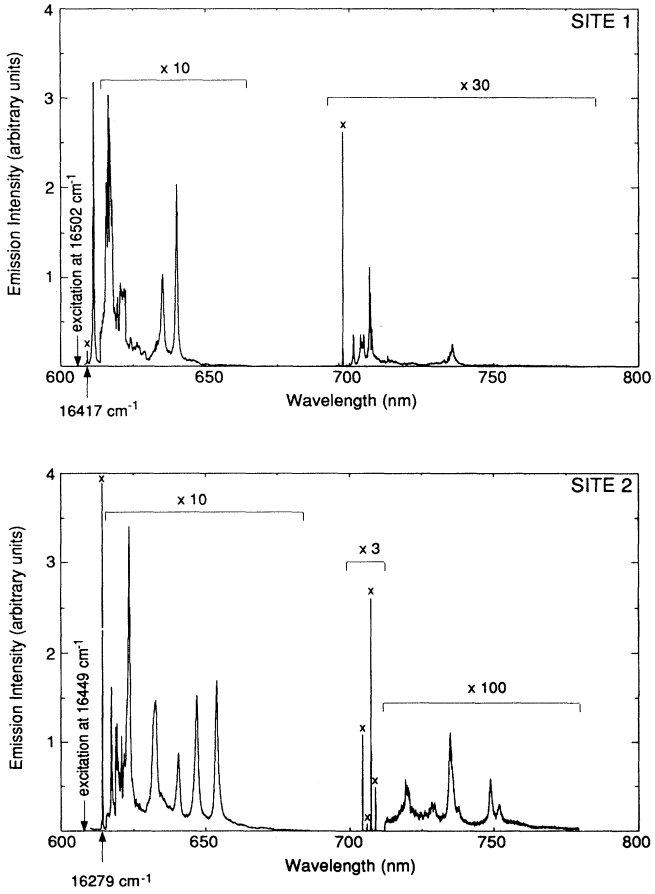

FIG. 2. The $^1D_2 \rightarrow {}^3H_4, {}^3H_5$ emission spectra at 20 K recorded by exciting the transition between the lowest crystal-field split components of the $^3H_4$ and $^1D_2$ levels. Emission to the next highest $^3H_4$ level is marked by an arrow. Crosses denote slit width limited features.

folds consisting of nine and three singlets, respectively. The $^1D_2 \rightarrow {}^3H_4, {}^3H_5$ emission spectra at 20 K, for each center are shown in Fig. 2. These spectra were recorded by exciting from the lowest component of the $^3H_4$ manifold to the lowest component of the $^1D_2$ manifold using the ring dye laser as an excitation source and a Jobin Yvon THR1000 double monochromator set to a resolution of 0.05 nm. The temperature was chosen to be 20 K so that no hole burning takes place. Several of the emission lines were slit width limited and these are indicated in Fig. 2. The splitting between the lowest two crystal-field levels of the ground state are important in analyzing nuclear-spin-lattice relaxation (see below) and are therefore marked in Fig. 2.

The center of the absorption zero-phonon lines corresponding to excitation from the lowest component of the $^3H_4$ manifold to the lowest component of the $^1D_2$ manifold, which are studied using hole burning and holography here, are 605.977 nm (site 1) and 607.933 nm (site 2). The inhomogeneous linewidths were measured as excitation spectra using a Coherent 899 autoscan dye laser and are 30 and 10 GHz (full width at half maximum), respectively. Emission was detected about 10 nm to the red with the monochromator slits wide open for both zero-phonon lines. The sample used in this study had peak absolute optical densities of 0.5 and 0.9 for the site 1 and 2 zero-phonon absorption lines, respectively.

IV. HOLE-BURNING SPECTRA

A comparison of the hole-burning spectra obtained for both sites using transmission and holography recorded at 1.6 K are shown in Fig. 3. Resonant hole widths of about 0.5 MHz, limited by laser jitter, were recorded for both sites. Signal to background ratios of the order of 10^3 and 10^4 were obtained for the holographic signals for site 1 and 2 resonant holes, respectively. The best ratio achieved in a dye-doped polymer such as chlorin doped poly (vinyl butyral) is of the order of 10^2 without frequency sweeping during burning.[16] Some of the nonresonant features are dwarfed by the very strong resonant hole in the Pr^{3+} holographic spectra. The signal-to-noise ratio of such features is still between 10–100 however. It is important to note that the holes shown in Fig. 3 are

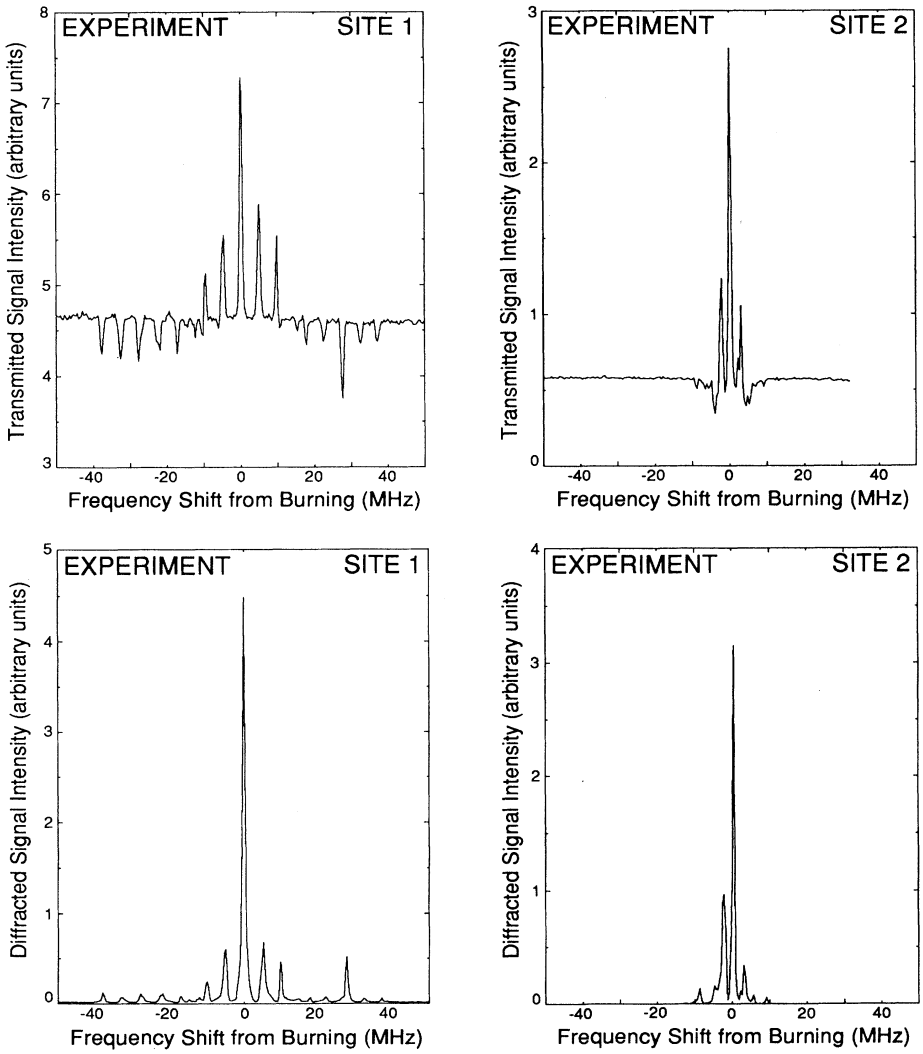

FIG. 3. The experimentally obtained hole spectra at 1.6 K measured in transmission (above) and holographically (below).

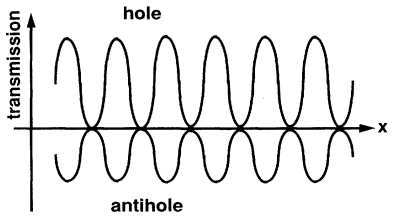

FIG. 4. Schematic illustration of the form of the gratings. The x direction is the horizontal axis of the sample surface. The resonant hole has a particular shape as determined by the interference pattern of the exciting radiation and the burning kinetics. All other spectral features are products of the resonant hole and must therefore have the same grating shape but with different amplitudes. Antiholes have a phase change of π however as the change in transmission is negative.

burnt with sufficiently high powers to allow a comparison of transmitted and diffracted signals to be made. When the power is reduced by a factor of 10 or more, strong hologram signals may still be observed though the hole spectrum may not be resolved from the transmitted beam.

The light diffracted by antiholes is π out of phase with that diffracted by the resonant hole and side holes. For each hole, the spatial position of the grating for all features is equivalent but the change in absorption is positive for antiholes and negative for the resonant and side holes causing the spatial phase of the grating for the two cases to be π out of phase (see Fig. 4).

Site 1 displays a typical hole spectrum for a system which exhibits spectral hole burning due to optical pumping between ground-state nuclear-spin levels.[11] The excited-state quadrupole splittings are given by the separation of the six side holes. In this case only four side holes are resolved, suggesting that the three excited-state Kramer's doublets are equally separated with splittings of 4.9 ± 0.3 MHz. The antihole structure was resolved by determining the ground-state quadrupole splittings by employing optical detection of magnetic resonance[17] (ODMR). Here, a radio-frequency magnetic field is applied by means of a copper coil wound around the sample. The radio frequency is scanned and the transmission of the sample monitored by a laser beam resonant with the electronic transition. When the radio frequency is resonant with a ground-state splitting, the hole is partly refilled and the transmitted beam intensity decreases. Strong signals were obtained for ground-state spin transitions but no signals were observed in the region of 4.9 MHz corresponding to excited-state splittings. The data are summarized in Table I.

TABLE I. Center frequencies and linewidths of transitions between ground-state Kramer's doublets for both sites as determined by optically detected magnetic resonance.

	Site 1		Site 2	
	Frequency (MHz)	Linewidth (kHz)	Frequency (MHz)	Linewidth (kHz)
$1/2\leftrightarrow3/2$	10.17	30	3.78	40
$3/2\leftrightarrow5/2$	17.28	70	4.92	80
$1/2\leftrightarrow5/2$	27.4	80	8.70	60

V. MODEL BASED ON TRANSMISSION SPECTRA

In order to model the observed diffraction efficiency site 1 was chosen due to the increased separation between spectral features. The absorptive and refractive index contributions to the hologram efficiencies have been calculated for a single Lorentzian spectral hole previously.[3] This analysis relies on substituting for the frequency, ω, and time, t, dependence of the zero and first-order contributions of the absorption, α, and refractive index, β, amplitude gratings into the following expression based on Kogelnik's coupled wave theory for thick holograms,[18]

$$\eta(\omega,t)=\frac{|E_d(\omega,t)|^2}{|E_r(\omega,t)|^2}$$
$$=e^{-2\alpha_0(\omega,t)d/\cos\theta}\left[\sinh^2\left[\frac{\alpha_1(\omega,t)d}{2\cos\theta}\right]+\sin^2\left[\frac{\beta_1(\omega,t)d}{2\cos\theta}\right]\right]. \quad (2)$$

The diffraction efficiency η is defined as being the ratio of the square of the complex field amplitude of the diffracted wave, $E_d(\omega,t)$, to that of the reference wave, $E_r(\omega,t)$, whilst d is the sample thickness and 2θ the angle between the burn beams.

In order to model the hologram spectra recorded here it is necessary to find expressions for the complex frequency dependence of the absorption and refractive index gratings. The interference between two spectrally adjacent holograms has been considered previously[19] and generalized to Z holes.[20]

The time evolution of the diffraction efficiency of such a series of spectra holes may be given by this modified version of Eq. (2),

$$\eta(\omega,t)=A_0^2(\omega,K_1,K_2,\ldots,K_z)\left[\sum_{i=1}^{Z}[A_{1i}^2(\omega,K_i)+B_{1i}^2(\omega,K_i)]\right.$$
$$+2\sum_{i=1}^{Z}\sum_{j=i+1}^{Z}[A_{1i}(\omega,K_i)A_{1j}(\omega,K_j)+B_{1i}(\omega,K_i)B_{1j}(\omega,K_j)]\cos(\varphi_i-\varphi_j)$$
$$\left.+2\sum_{i=1}^{Z}\sum_{j=i+1}^{Z}[B_{1i}(\omega,K_i)A_{1j}(\omega,K_j)-A_{1i}(\omega,K_i)B_{1j}(\omega,K_j)]\sin(\varphi_i-\varphi_j)\right]. \quad (3)$$

The first line of the expansion describes the contribution of each of the Z gratings individually, where the normalized efficiency of the ith hologram, η_i, is given by $A_{1i}^2(\omega,K_i)+B_{1i}^2(\omega,K_i)$, and $A_0(\omega,K_1,K_2,\ldots,K_Z)$ describes the damping due to the unmodulated part of the absorption coefficient. The final two lines of Eq. (3) describe the contributions due to interference between each pair of gratings, which are burnt with a spatial phase difference, $\varphi_i-\varphi_j$.

The terms A_{1i} describe the first-order contributions of the absorption gratings and B_{1i} represent the first-order contributions of the refractive index gratings and are simply derived from α and β by approximating the hyperbolic sine and sine functions in Eq. (2) to be the arguments of the functions. For hole depths of 30%, as typically used in this study, the approximation causes an error of less than 1%. The full expressions are

$$A_0(\omega,K_1,K_2,\ldots,K_Z)=\exp\left[-\frac{\alpha_0(\omega,K_1,K_2,\ldots,K_Z)d}{\cos\theta}\right],$$
$$A_{1i}(\omega,K_i)=\frac{\alpha_{1i}(\omega,K_i)d}{2\cos\theta}, \tag{4}$$
$$B_{1i}(\omega,K_i)=\frac{\beta_{1i}(\omega,K_i)d}{2\cos\theta}.$$

As α_0 is a quantity derived from the measured transmission spectra and α_1 and β_1 are calculated from this, their values are initially calculated as intensities and then converted to amplitudes before substitution into Eq. (4).

The frequency-dependent burning kinetics are represented by K. In former studies K evolved steadily with time as the hole became deeper. In the case of hole burning through optical pumping, the hole depth is quickly established as being the equilibrium between pumping and spin-lattice relaxation. Therefore, after equilibrium is established, K is a function of burn power. As we are working with laser limited linewidths, saturation broadening of the lines does not occur until relatively high powers (see above) and we neglect this effect here.

To utilize Eq. (3) for the hole pattern shown in Fig. 3 it would be necessary to sum the contributions of all the predicted seven holes and 42 antiholes. As the precise pumping dynamics are not known for this system (see below) we start by using the transmission hole pattern as the basis for the hole-burning kinetics. The gratings corresponding to holes and antiholes have a relative phase of π as the antiholes represent photoproduct and the holes educt (see Fig. 4). Consequently, $\varphi_i-\varphi_j=0$ or π and the last term in Eq. (3) is always zero. Furthermore, $\cos(\varphi_i-\varphi_j)$ is always ±1. To take account of this and in order to simplify Eq. (3) the A_{1i} and B_{1i} terms are defined as being positive for holes and negative for antiholes to give

$$\eta(\omega,t)=A_0^2(\omega,K_1,K_2,\ldots,K_Z)\left\{\left[\sum_{i=1}^{Z}A_{1i}(\omega,K_i)\right]^2+\left[\sum_{i=1}^{Z}B_{1i}(\omega,K_i)\right]^2\right\}. \tag{5}$$

It is convenient to substitute the absorption and refractive index contributions in terms of the population grating, N. The zero- and first-order absorption and first-order refractive index grating amplitude contributions, α_0, α_{1i} and β_{1i}, are given by

$$\alpha_0(\omega,K_1,K_2,\ldots,K_Z)=S\int_0^\infty N_0(\omega,K_1,K_2,\ldots,K_Z)G(\omega,\sigma)d\omega,$$
$$\alpha_{1i}(\omega,K_i)=S\int_0^\infty N_{1i}(\omega,K_i)G(\omega,\sigma)d\omega, \tag{6}$$
$$\beta_{1i}(\omega,K_i)=S\int_0^\infty N_{1i}(\omega,K_i)D(\omega,\sigma)d\omega,$$

where S is the integrated absorption cross section, $N_0(\omega,K_1,K_2,\ldots,K_Z)$ and $N_{1i}(\omega,K_i)$ are the zero- and first-order population grating contributions, and $G(\omega,\sigma)$ and $D(\omega,\sigma)$ represent the Gaussian and corresponding dispersion line shapes of the spectral hole. A Gaussian function is chosen here as the holes are laser linewidth limited.

The diffraction efficiency as given by Eq. (5) therefore contains two sums of integrals. The integral and summation signs may be swapped and the calculation performed as the integral of a sum:

$$\eta(\omega,t)=S\left[\frac{d}{\cos\theta}\right]^2\exp\left[-\frac{2d}{\cos\theta}\left[S\int_0^\infty N_0(\omega,K_1,K_2,\ldots,K_Z)G(\omega,\sigma)d\omega\right]\right]$$
$$\times\left\{\left[\int_0^\infty\sum_{i=1}^{Z}N_{1i}(\omega,K_i)G(\omega,\sigma)d\omega\right]^2+\left[\int_0^\infty\sum_{i=1}^{Z}N_{1i}(\omega,K_i)D(\omega,\sigma)d\omega\right]^2\right\}. \tag{7}$$

This is particularly convenient as the population grating may be simply calculated from the measured transmission of the sample. In this way, the entire hole spectrum may be considered as a single frequency-dependent grating. Expressions for $N_0(\omega,K)$ and $N_1(\omega,K)$ have been given previously[3] as

$$N_0(\omega,K)=N(0)e^{-K}I_0(K),$$
$$N_1(\omega,K)=2N(0)e^{-K}I_1(K), \tag{8}$$

where I_0 and I_1 are Bessel functions corresponding to the shape of the grating determined by the hole-burning dy-

namics contained in K. To extend this to the case of a multiple grating consisting of one resonant and many nonresonant parts it is necessary to treat the zero- and first-order components differently. The zero-order population grating, N_0, is calculated by summing the change in population, for gratings of different depths, and subtracting this from the initial population, $N(0)$. The first-order grating is merely the sum of the contributions from each feature,

$$N_0(\omega,K_1,K_2,\ldots,K_Z) = N(0)\left[1-\sum_{i=1}^{Z} f_i[1-(e^{-K_i'}I_0(K'))]\right],$$
$$N_1(\omega,K_1,K_2,\ldots,K_Z)=2N(0)\sum_{i=1}^{Z} f_i e^{-K_i'} I_1(K') . \quad (9)$$

The population grating for the resonant hole is determined by the equilibrium between burning and refilling. The dynamics of the hole-burning process may therefore be represented by a single time-independent but frequency-dependent term, K'. The side and antiholes are the direct product of the resonant hole burning and must therefore have population gratings with identical shapes but different magnitudes, given by f_i. This is an approximation which assumes transition probabilities between each ground- and excited-state Kramers doublet are equal. The K_i' terms in the summations are taken to be identical except for the center frequency of each contribution.

The values of f_i may be obtained directly from the transmission spectrum. From a comparison of Eqs. (7) and (9) it can be seen that each feature makes a contribution to the change in the zero-order absorption coefficient, α_0, in proportion to f_i. The absorption coefficient may be simply obtained from the transmission spectrum. In our calculation K_i' is taken to be a Gaussian with $\sigma=0.4$ MHz and center frequencies determined by the ODMR data. The amplitudes of each K_i' are identical but may all be varied together to account for the burning power used. It is now possible to calculate N_0 and N_1 and from these the α_{1i} and β_{1i} terms. The experimental data for α_0 is used to normalize S and $N(0)$ so that the absolute values of α_{1i} and β_{1i} may be determined. The hologram efficiency may then be simply calculated.

The result of the simulation is shown in Fig. 5. A good fit to the experimental data is observed. Variations between experiment and theory may be accounted for by laser jitter and drift which cause the frequency scan to be somewhat nonlinear, causing the very narrow spectral features to be resonant with the probe beam for varying periods of time. In positions where holes and antiholes overlap it is likely that the contribution of each is underestimated using this technique and further discrepancies occur at these frequencies.

VI. MODEL BASED ON BURNING KINETICS

To model the holographic efficiency from burning kinetics based solely on the quantum mechanics of the system, an *ab initio* calculation of the burning kinetics must be performed based on the absorption and relaxation probabilities of the transitions between different nuclear quadrupole levels of the ground- and excited-state Kramer's doublets. As relaxation may take place through a complex route via other electronic singlets, and as the extent of excited-state nuclear-spin relaxation is not known, a calculation which takes account of only the quadrupole wave functions of the resonant singlet states is likely to be poor. For instance, an attempt to assign the sign of E [Eq. (1)] based on the intensities of spectral hole features in the $LaF_3:Pr^{3+}$ system[12] was shown to be wrong by a study which employed Raman heterodyne detection of magnetic resonance.[21]

Here a useful approximation is made. The burning process is considered to be equivalent for each of the nine transitions between ground- and excited-state Kramer's doublets but selection rules are applied for the read process. As the signs of D and E in Eq. (1) are not initially known, several possible hole patterns result from this technique. By selecting the pattern which most closely

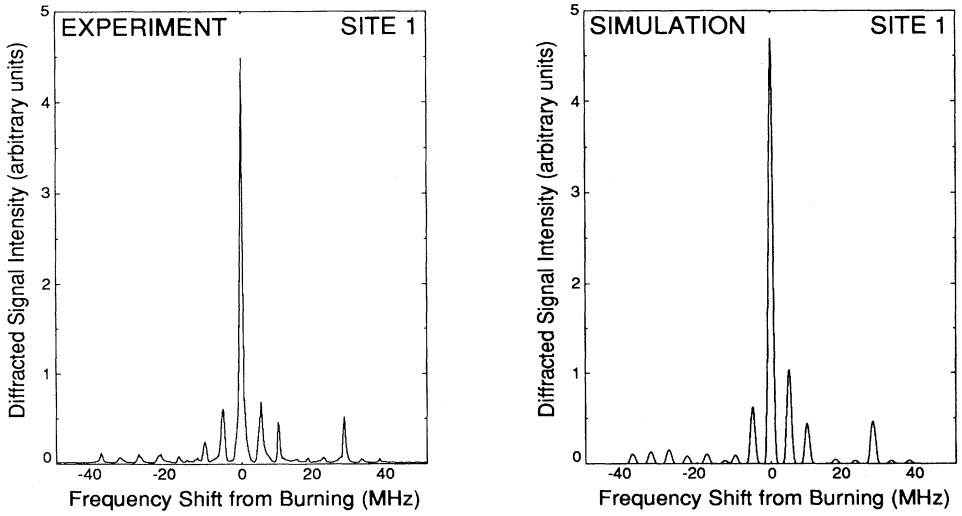

FIG. 5. The hologram efficiency for site 1, experimental (left) and as calculated using the experimentally measured transmission spectrum (right).

resembles the experimentally measured spectrum the signs of D and E may be determined. The transmitted hole spectrum obtained in this way is shown in Fig. 6 (upper). Here, the ground-state splittings from Table I and the excited-state splittings from the hole spectra are used. By assuming the lowest Kramer's doublet of the ground state to be the perturbed $|5/2\rangle$ state and the lowest Kramer's doublet of the excited state to be the perturbed $|1/2\rangle$ state, a good qualitative fit to the transmission spectrum [Fig. 3 (upper left)] is obtained. From this information the sign of the quadrupole parameters given in Eq. (1) have been deduced and are given in Table II. Using this model, 21 of the 22 prominent features appear at their experimentally measured frequencies and the order of magnitude of the relative size of the features are reproduced. The exceptions to the success of this simple model are the antihole predicted at $+6$ MHz which appears at -6 MHz and the antihole which is predicted at -20 MHz but which appears as a side hole. Both of these features are associated with pumping between the perturbed $|3/2\rangle$ and $|5/2\rangle$ ground states but the precise reason for this behavior is not understood.

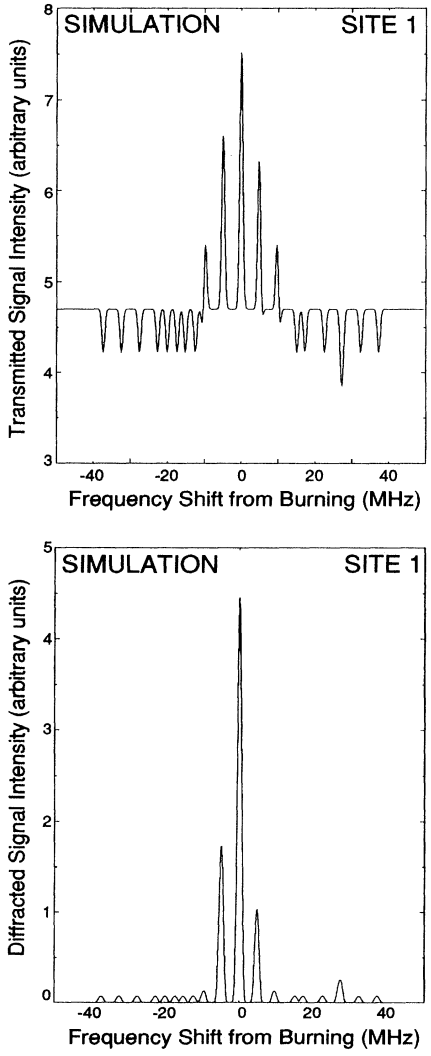

FIG. 6. The transmission hole spectrum (above) and the hologram efficiency (below) calculated on the basis of a consideration of selection rules.

TABLE II. Values for D and E [see Eq. (1)] as determined by optically detected magnetic resonance and spectral hole-burning measurements.

	Site 1		Site 2
	Ground state	Excited state	Ground state
D (MHz)	-4.443	$+1.39$	± 1.32
E (MHz)	-0.503	$+0.46$	± 0.31

The hologram efficiency may also be calculated from the hole spectrum shown in Fig. 6(a). The process of converting the calculated transmitted intensity to the calculated diffracted signal is identical to that described above for the experimental data. The resulting spectrum is shown in Fig. 6(b). Again, a reasonable fit to the data is obtained though lack of knowledge of the precise optical pumping kinetics prevents the fit from being perfect.

VII. STARK EFFECT

The high signal-to-noise ratio associated with the holographic hole-burning spectra make this technique ideal for an investigation of pseudo-Stark effects. As both sites have C_1 point symmetry,[15] all crystal-field levels have Γ_1 irreducible representations and the expectation value of the electric dipole moment is always nonzero, $\langle \Gamma_1 | \mu_{x,y,z} | \Gamma_1 \rangle > 0$. Figure 7 shows the experimental hole spectra as surface and contour plots for both sites as a function of frequency and electric field. The regions with large amounts of structure close to the burn frequency and electric field correspond to a large number of constructive and destructive interference effects that take place as holes and antiholes, which are π out of phase with each other, shift in different directions at different rates.

From the data shown in Fig. 7 and from the projection of the crystal structure of Y_2SiO_5 on the ac plane it is possible to assign the spectroscopically distinguished sites to those determined through x-ray analysis.[15] For the site previously referred to as Y_1 in (Ref. 15) there are four inequivalent orientations relative to the b axis. For the Y_2 site only two such sites exist. The site 1 hole appears to split into two components whereas the site 2 hole splits into four components. The previously named Y_1 and Y_2 sites are thus ascribed to those referred to here as site 2 and site 1, respectively. Upon closer inspection it can be seen that each Stark-split component of the site 1 holes is itself split. This is ascribed to the 13° misalignment of the crystal from the [0,1,0] direction which causes differently oriented sites, which are symmetric about the b axis, to become inequivalent with respect to the externally applied electric field. In this preliminary investigation the crystal was fixed in one experimental orientation

and so precise calculations of dipole moment differences cannot be made though the splittings suggest that the order of magnitude is similar to that measured previously in the $LaF_3:Pr^{3+}$ system.[22]

Several technological applications[7,8] rely on the interference between Stark-split components of spectral holes burnt as holograms.[23] Crystalline hosts offer the advantage that Stark-split components of spectral holes do not broaden as the electric field is varied from the burn value resulting in strong interference between components of different holes. The lack of structure associated with site 2 makes it preferable for a demonstration of this effect (Fig. 8). The holes were burnt with zero spatial phase difference, that is both burn gratings had identical positions, in order to observe constructive interference between the resonant hole features. As noted above, the actual interference behavior is complicated by the presence of the antiholes which have gratings π out of phase with holes and side holes. Nevertheless, four positions of constructive interference are observed in the surface plot in a section through $E=0$. Four further areas of constructive interference may be observed at $E=\pm 0.35$ kV/cm, which correspond to the positions at which Stark components from different holograms with different splitting rates overlap. Here the principles of interference between holograms burnt as spectral holes in crystals are demonstrated but the application of this technique would be better suited to a material for which nonresonant structure does not appear in the vicinity of the resonant hole and for which the splitting may be limited to two

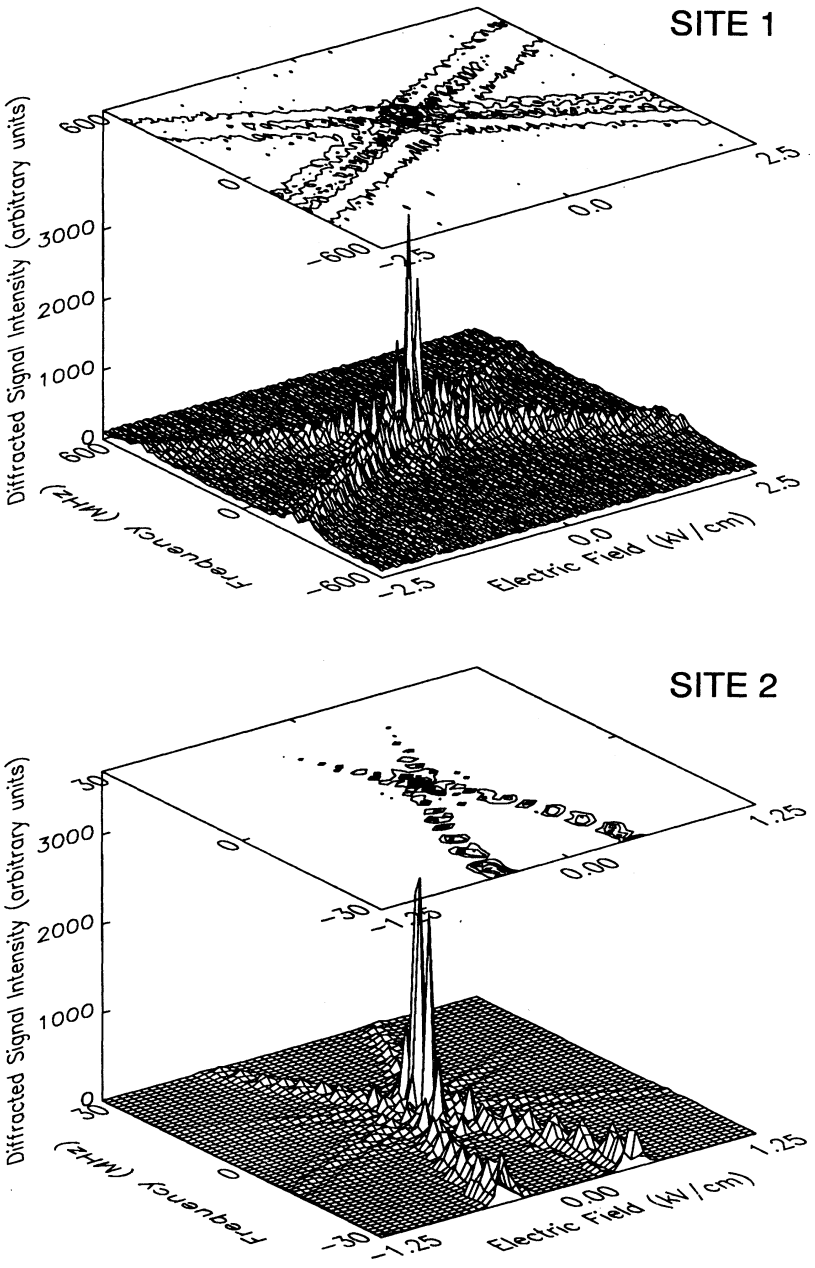

FIG. 7. The splitting of a single spectral hole as a function of externally applied electric field detected holographically. The diffracted intensity is plotted as a surface and contour plot as a function of reconstruction frequency and applied electric-field strength. The features are weaker at higher frequencies due to the time decay of the hole during data acquisition. Zero frequency refers to the burn position near to the center of the zero-phonon line. The slight shift from zero frequency in the readout and the nonlinearity of the splittings is attributable to laser drift.

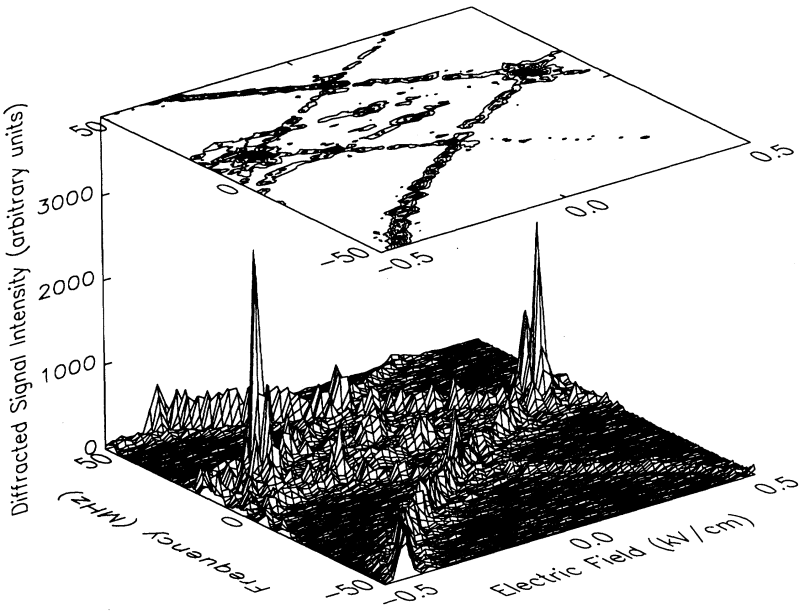

FIG. 8. Interference between Stark-split components of spectral holes burnt as holograms at ±0.4 kV/cm for site 2 plotted as for Fig. 7. Four areas of constructive interference may be observed in a cut through the figure for $E_s=0$. Two additional pairs may be observed at ±3 kV/cm. Zero frequency refers to the burn position near to the center of the zero-phonon line. The slight shift from zero frequency in the readout and the nonlinearity of the splittings is attributable to laser drift.

features. A suitable candidate may be the 607-nm color center in NaF.[24]

VIII. NUCLEAR-SPIN-LATTICE RELAXATION

A previous hole-burning study of a crystalline rare-earth impurity system, $LaF_3:Pr^{3+}$, determined three mechanisms to be responsible for the time decay of the hole.[25] For this system, a temperature-dependent Orbach process caused by phonon absorption to the first electronic level about the ground state dominates the hole refilling above about 3.5 K. Cross relaxation between single Pr ions and three surrounding ^{139}La nuclei make a concentration and temperature-independent contribution. Finally, Pr ions which have been removed from resonance may return to their original nuclear-spin level through a spin flip-flop with a neighboring Pr ion. If the second Pr ion is not in resonance with the laser before or after the cross-relaxation process takes place the hole will be refilled. Such a contribution is temperature independent but dependent on impurity concentration.

The experimental arrangement used here required that holography be performed in pumped liquid helium at 1.6 K. In order to investigate the temperature dependence of the hole decay transmission spectra were recorded between 1.6–16 K. The decay of the resonant hole for both sites is illustrated in Fig. 9. To within experimental error there is no difference between the decays at 1.6 and 4.2 K. Holes burnt in the zero-phonon line of site 1 decayed marginally more slowly than those in site 2. For site 1, a significant decrease in hole lifetime was observed at 6 K, whilst no holes could be observed using the usual technique at 8 K. By abruptly decreasing the laser intensity and observing the decay of the transmitted beam the holes were found to completely refill in less than 1 s, the

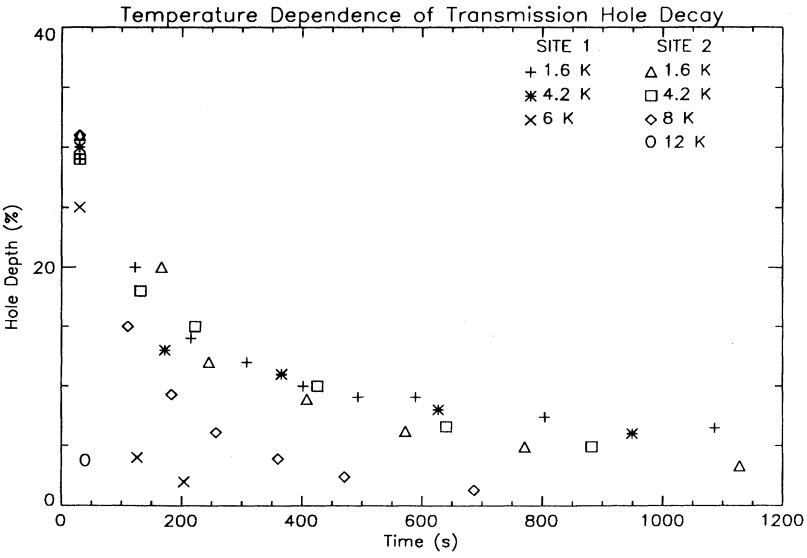

FIG. 9. The time decay of holes burnt in sites 1 and 2 (open symbols) at various temperatures as indicated.

precise time depending on the depth of the hole burnt. For site 2, a small decrease in lifetime is observed at 8 K and a fast decay at 12 K. At 16 K no hole burning could be observed. These data fit very well to the resonant two-phonon Orbach process model proposed previously to explain the hole decay data for the $LaF_3:Pr^{3+}$ system.[25] This process involves the first excited crystal-field level of the $^3H_4$ manifold and predicts a temperature dependence proportional to $\exp(-E_1/kT)$ where k is Boltzmann's constant and T is the absolute temperature. The energy separation between the two lowest crystal-field levels is given by E_1 and is 85 and 170 cm^{-1} (see Fig. 2) for sites 1 and 2, respectively. Hole refilling due to the Orbach process should therefore begin to dominate for site 1 at a temperature relative to that for site 2 in proportion to the ratio of the respective values of E_1, that is at one half the temperature. This can be seen by comparing the hole decay of site 1 at 4.2 K and site 2 at 8 K and further by comparing the hole decay of site 1 at 6 K and site 2 at 12 K. Though the decay is marginally faster for site 2, as at lower temperatures, the close similarity strongly suggests that the Orbach process does account for the temperature dependence of hole refilling in this system. For the $LaF_3:Pr^{3+}$ system[25] hole refilling begins to be dominated by the Orbach process at about 3.5 K, a lower temperature than for either site in $Y_2SiO_5:Pr^{3+}$ but also in proportion to the value for E_1 of 57 cm^{-1}.

The contribution of phonon-induced relaxation processes to hole refilling at 1.6 K may therefore be assumed to be negligible. Furthermore, the interaction between host and impurity ions is expected to be weak as evidenced by the extremely long dephasing time measured for the $^5D_0$-$^7F_0$ transition of Eu^{3+} ions in Y_2SiO_5.[10] The hole-refilling process is therefore expected to be dominated by Pr-Pr interactions at 1.6 K. The data shown in Fig. 9 do not fit to a single exponential. This is to be expected as the relaxation between the three levels progresses at different rates for different spin transitions. A technique to extract the three rate constants has been applied to the $LaF_3:Pr^{3+}$ system.[25] Application of a radio-frequency magnetic field resonant with any of the ground-state quadrupole splittings causes the populations of the coupled levels to be equalized. If hole burning is conducted while the field is on, the hole spectrum should be restrict-

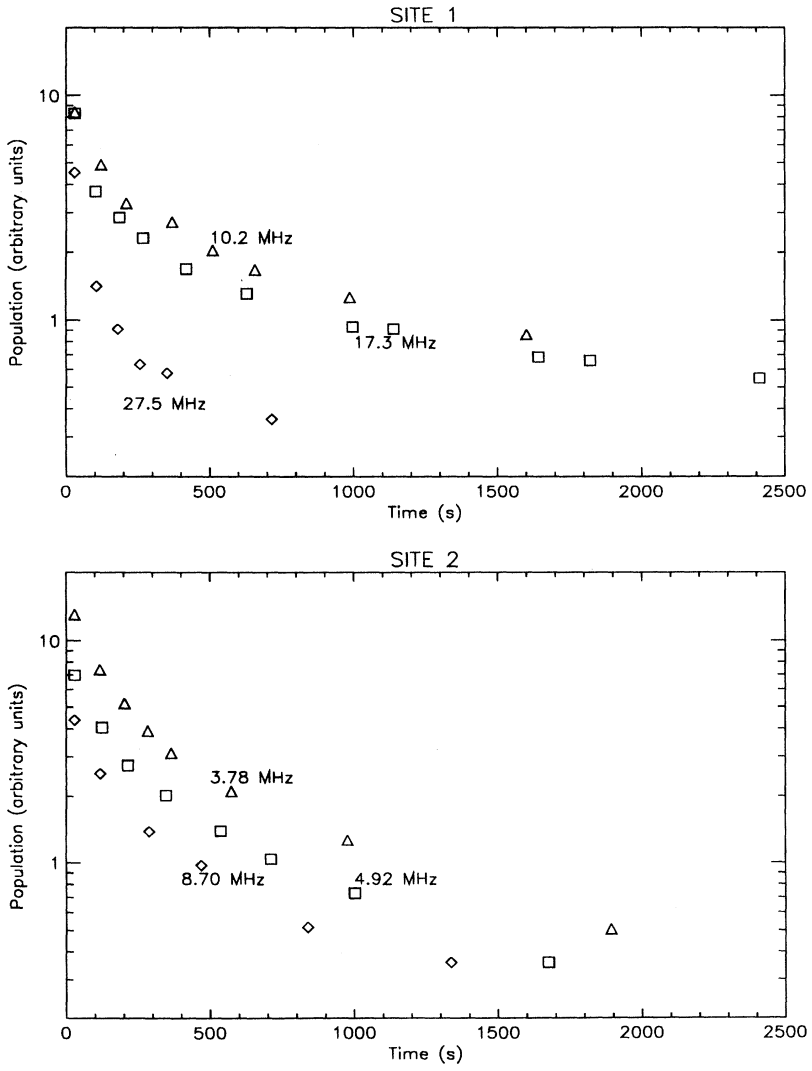

FIG. 10. The time decay of the population of ions in nonequilibrium nuclear-spin states derived from spectral holes burnt as holograms. The experiment was performed while the sample was irradiated with a saturating radio-frequency field resonant with each of the three ground-state quadrupole splittings, the frequencies of which are indicated.

ed to changes of spin between a magnetically coupled level and the uncoupled one. Similarly, if the hole decays under the same conditions, relaxation is between only the uncoupled level and the coupled levels, resulting in a single exponential decay.

The holographic technique is ideal for such an investigation as the hole depth may be measured over several lifetimes with high accuracy. At the end of the burning period the grating has a definite spatial form, determined by the burning kinetics. Nuclear-spin transitions for each ion now proceed independently of position within the grating and so a time-dependent expression for the decay may be inserted as a product term in the expression for population [Eq. (9)]. This is in contrast to the time dependence of the growth of holographic efficiency during burning studied previously,[3] where molecules undergo transformations at different rates depending on their orientation within the sample. Nevertheless, to study nuclear-spin-lattice relaxation the decay of the population must be derived from the holographic efficiency. To do this only the resonant hole need be considered and Eq. (3) is applied to the case of a single hole ($Z=1$). The B_{11} term is set to zero as the line shape is dispersive and therefore always zero at the resonant frequency. The expression for holographic efficiency thus reduces to

$$\eta = A_0^2 A_{11}^2 \ . \tag{10}$$

By considering Eq. (5) it can be seen that, at the center frequency of the resonant hole, A_{11} is proportional to the population. The population is thus proportional to the square root of the holographic efficiency after correction for absorption by the unmodulated part of the absorption grating, A_0. This correction factor is proportional to the transmission of the sample at the burn frequency, a parameter which we measure simultaneously in these experiments. The accuracy of the holographic technique is not undermined by using the transmission data because as the transmission hole becomes weak, and consequently inaccurate, the correction term becomes almost constant. The hole width does not need to be considered as it remains constant as determined by the laser linewidth.

The decay of the population for both sites was studied. Holes were burnt and read whilst scanning the radio frequency across the whole of the spin transition inhomogeneous linewidth for all three transitions separately. The data are plotted on a logarithmic-linear scale in Fig. 10. In all six cases a straight line is not observed. The decay of the population is not exponential. This supports the prediction that the hole refilling is dominated by guest-guest interactions. An exponential hole decay would be expected for hole refilling caused by phonon or guest-host interactions as such processes take place independently of the position of the impurity ion within the lattice. As the impurity ion concentration is very low there will be a large variation in the distances between neighboring praseodymium ions and consequently a large variation in coupling constants for spin-spin cross relaxation. This process should therefore take place at different rates for impurity ions, which are coordinated differently with respect to surrounding impurity ions, resulting in the nonexponential decay observed. Calculations intended to substantiate these claims will be given in a further publication.[26]

IX. CONCLUSION

The techniques of spectral hole-burning and holography have been applied to a crystalline material and shown to be a method by which resonant and nonresonant spectral features may be detected with very high signal-to-noise ratios. This effect has been modeled for the general case of a hole accompanied by local spectral structure for which holes and antiholes create gratings π out of phase with each other. This theory has been combined with the data obtained by detecting the hole spectrum in transmission to simulate the diffracted spectrum. Furthermore, both transmitted and diffracted hole spectra were successfully modeled by applying selection rules to the read process only.

Applications of this technique have been demonstrated. The pseudo-Stark splitting of a spectral hole in an externally applied electric field was measured and this enabled the two spectroscopically distinguished sites to be matched to those determined earlier by x-ray diffraction. The refilling of holes burnt and read in the presence of a saturating radio-frequency field resonant with a quadrupole splitting was also investigated using this technique and shown to be dominated by Pr-Pr nuclear-spin cross relaxation.

The high signal-to-noise ratio associated with this technique suggests it could be of use in studying a wide range of effects in a wide range of hole-burning materials. Though this particular material is unlikely to be of technological use, it has been shown that applications already demonstrated in dye-doped polymers will also work in crystalline materials. The associated increase in the signal-to-noise ratio and the strong interference between Stark-split components of spectral holes suggest that crystalline materials will in fact be more suitable for molecular computing applications than polymers.

ACKNOWLEDGMENTS

We are indebted to Dr. Masa Mitsunaga of NTT, Japan for the gift of the sample and for his preliminary measurements. We thank Dr. Alois Renn for advice on theoretical and practical aspects of spectral hole burning and holography, Jürg Forrer, Bruno Lambillotte, and Markus Traber for technical assistance, Jaroslav Hajfler for x-ray-diffraction measurements and Professor Arthur Schweiger for the loan of radio-frequency equipment. One of us (K. H.) thanks M. Krotthammer for stimulating discussions. This work was supported by the Swiss National Science Foundation.

*Present address: Department of Physics and Applied Physics, John Anderson Building, University of Strathclyde, Glasgow G4 ONG, United Kingdom.
†Present address: Institute of Physical Chemistry, University of Fribourg, Perolles, CH-1700 Fribourg, Switzerland.

[1]*Persistent Spectral Hole Burning: Science and Applications,* edited by W. E. Moerner (Springer, Berlin, 1988).
[2]K. Holliday and U. P. Wild, in *Molecular Luminescence Spectroscopy: Methods and Applications Part III,* edited by S. Schulman (Wiley, New York, 1993), Chap. 5.
[3]A. J. Meixner, A. Renn, and U. P. Wild, J. Chem. Phys. **91**, 6728 (1989).
[4]D. Redman, S. Brown, and S. C. Rand, J. Opt. Soc. Am. B **9**, 768 (1992).
[5]A. Renn, S. E. Bucher, A. J. Meixner, E. C. Meister, and U. P. Wild, J. Lumin. **39**, 181 (1988).
[6]E. Vauthey, K. Holliday, C. Wei, A. Renn, and U. P. Wild, Chem. Phys. **171**, 253 (1993).
[7]U. P. Wild, S. Bernet, B. Kohler, and A. Renn, Pure Appl. Chem. **64**, 1335 (1992).
[8]S. Bernet, A. Renn, B. Kohler, and U. P. Wild, in *Spectral Hole Burning and Luminescence Line Narrowing: Science and Applications,* edited by U. P. Wild, Opt. Soc. Am. Tech. Digest Series No. 22 (OSA, Washington, 1992), p. 218.
[9]R. Yano, M. Mitsunaga, and N. Uesugi, J. Opt. Soc. Am. B **9**, 992 (1992).
[10]R. Yano, M. Mitsunaga, and N. Uesugi, Opt. Lett. **16**, 1884 (1991).
[11]R. M. Macfarlane and R. M. Shelby, in *Spectroscopy of Solids Containing Rare-Earth Ions,* edited by A. A. Kaplyanskii and R. M. Macfarlane (North-Holland, Amsterdam, 1987), Chap. 3.
[12]L. E. Erickson, Phys. Rev. B **16**, 4731 (1977).
[13]M. A. Teplov, Zh. Eksp. Teor. Fiz. **53**, 1510 (1967) [Sov. Phys. JETP **26**, 872 (1968)].
[14]T. P. Das and E. L. Hahn, Solid State Phys., Supp. 1 (1958).
[15]A. M. Tkachuk, A. K. Przhevusskii, L. G. Morozova, A. V. Poletimova, M. V. Petrov, and A. M. Korovkin, Opt. Spectrosk. **60**, 288 (1986) [Opt. Spectros. (USSR) **60**, 176 (1986)].
[16]S. Bernet, B. Kohler, A. Rebane, A. Renn, and U. P. Wild, J. Opt. Soc. Am. B **9**, 987 (1992).
[17]L. E. Erickson, Opt. Commun. **15**, 147 (1977).
[18]H. Kogelnik, Bell System Tech. J. **48**, 2909 (1969).
[19]A. Renn, A. J. Meixner, and U. P. Wild, J. Chem. Phys. **92**, 2748 (1990).
[20]C. De Caro, Ph.D thesis, ETH Zürich Nr. **9526**, 128 (1991) (in German).
[21]M. Mitsunaga, E. S. Kintzer, and R. G. Brewer, Phys. Rev. B **31**, 6947 (1985).
[22]R. M. Shelby and R. M. Macfarlane, Opt. Commun. **27**, 399 (1978).
[23]A. Renn, A. J. Meixner, and U. P. Wild, J. Chem. Phys. **93**, 2299 (1990).
[24]R. T. Harley and R. M. Macfarlane, J. Phys. C **16**, 1507 (1983).
[25]R. M. Shelby, R. M. Macfarlane, and C. S. Yannoni, Phys. Rev. B **21**, 5004 (1980).
[26]M. Croci, U. P. Wild, and K. Holliday (unpublished).